Sustainable and green approach for api 5L pipeline steel acidic corrosion inhibition using agro-industrial waste: Experimental and theoretical.

metals

MDPI

Article

Sustainable and Green Approach for Api 5L Pipeline Steel Acidic Corrosion Inhibition Using Agro-Industrial Waste: Experimental and Theoretical

Abimbola Patricia Popoola, Alice Osheiza Alao * and Omotayo Sanni

Department of Chemical, Metallurgical and Materials Engineering, Tshwane University of Technology, Staatsartillerie Road, Private Bag X680, Pretoria 0001, South Africa; opoolaapi@tut.ac.za (A.P.P.); sannio@tut.ac.za (O.S.)

* Correspondence: sweetdamsel08@gmail.com

Abstract: Currently, the use of synthetic inhibitors in preventing corrosion is destructive to the environment; therefore, natural inhibitors might be an alternative and innovative solution to this challenge, owing to their sustainability. Herein, wasted avocado seed extract was examined as a sustainable and green inhibitor for API 5L X65 pipeline steel at an ambient temperature using the gravimetric analysis, the potentiodynamic polarization curve, and linear polarization resistance techniques. The inhibitor's chemical characterization was carried out with Fourier-transform infrared spectroscopy (FTIR), and the morphological characterization was carried out by detailed scanning electron microscopy and energy-dispersive X-ray spectroscopy (SEM/EDX). The result showed that the extract decreased the corrosion rate by retarding the cathodic and anodic electrochemical reactions, with a maximum efficiency of 88% at 5 g/L. The extract was adsorbed physically onto the X 65 steel following the Langmuir adsorption isotherms. The electrochemical studies showed that the agro-waste was a mixed-type inhibitor. The SEM image of the X65 steel with the extract showed thin film formation on the steel surface. The extract can be substituted for synthetic inhibitors, which are toxic, scarce, and costly.

Keywords: avocado seed extract; acid corrosion; pipeline steel; sustainable inhibitor; corrosion inhibition

Citation: Popoola, A.P.; Alao, A.O.; Sanni, O. Sustainable and Green Approach for Api 5L Pipeline Steel Acidic Corrosion Inhibition Using Agro-Industrial Waste: Experimental and Theoretical. *Metals* **2023**, *13*, 1155. https://doi.org/10.3390/met13071155

Academic Editors: David M. Bastidas and Dake Xu

Received: 6 May 2023
Revised: 13 June 2023
Accepted: 16 June 2023
Published: 21 June 2023

1. Introduction

API 5L X65 steel is utilized mostly as a piping material in the oil and gas industry, due to its excellent mechanical properties, such as good corrosion resistance, good fatigue resistance, good toughness, and high strength. However, in the oil and gas sectors, the operational activity where pipeline steel is highly susceptible to corrosion has a negative impact on the environment and economy [1]. Most industries use acid solutions for the maintenance, preservation, and cleaning processes. These activities lead to the metal degrading. Corrosion leads to a decrease in the steel's mechanical properties, causing a reduction in thickness, strength, and tenacity, as well as material degradation [2], thereby resulting in an approximately 80–90% failure in this sector. However, methods for controlling or improving such an occurrence has become a research focus. Among different methods, one of the cheapest and most practical ways to protect metal against corrosion is the application of an inhibitor [3,4]. Effective organic compounds utilized as corrosion inhibitors are generally compounded with an electronegative functional group, such as N, O, S, or P, that have a double bond in their molecule. Nevertheless, synthetic compounds may be harmful to human health and have some negative consequences for the environment. Scientists are developing a natural inhibitor that is easily obtainable, environmentally friendly, and cheap. Therefore, in the oil and gas sector, the green corrosion inhibitor has become an important area of focus. Plant extract is rich in natural chemical sources, can be extracted by

a simple procedure, decomposes in nature easily, and is inexpensive [5]. Different natural extracts have been reported to have good inhibition efficiency such as the extract of cocoa seed [6,7], *Coromandelica* leaf extract [8], papaya leaf extract [9], olive extract [10], coconut leaf extract [11], cumini leaf extract [12], and *Peumusboldus* leaf extract [13].

The *Persea Americana* (avocado) is usually utilized for culinary purposes and, in the cosmetic sector, has had great importance in the culture and diet of several countries for thousands of years [14]. Avocado is found basically globally. According to the Major Tropical Fruits–2019 Preliminary Markets Result given by the FAO (Food and Agriculture Organization of the United Nations), the *Persea Americana* is anticipated to attain 29% of the total world trade in major tropical fruits, only coming behind pineapple (46%) [15]. Despite the numerous benefits of the consumption and utilization of the fruit, the peel and the seed are not fully utilized by consumers or in the industry. Therefore, those residues are generally discarded. Avocado seed waste has not been optimally utilized. Hence, transforming avocado seed, which is originally waste, into a high-value product is crucial. The avocado seed contains flavonoids, phenolic, sesquiterpenoids, tannins, triterpenoids, quinones, monoterpenoids, and saponins, with 13.25% starch and 13.6% tannins [16]. The potential effect of the avocado seed as a corrosion inhibitor, owing to its chemical compounds, can be studied. Avocado seeds are non-toxic, biodegradable, sustainable, and readily available from renewable sources.

Agricultural bio-waste has lately gained substantial attention as a corrosion inhibitor for engineering materials, as previously reported in literature [17–19]. Avocado seed contains aromatic rings and heteroatoms, indicating that it can be used as a high-performance and sustainable corrosion inhibitor. Other researchers have also reported the influence of avocado oil and seed for other materials [20–25]. Thus, this study was designed to study the potential of avocado seed extracts as a green corrosion inhibitor that is environmentally friendly, nontoxic, and cheap for API 5L X65 steel usually used for pipelines in 1 M H_2SO_4 solution.

2. Experimental Procedure

2.1. Solution and Sample Preparation

API 5L X65 pipeline steel, with the chemical composition presented in Table 1, was used in this study. The steel sheet was mechanically cut into a size of 2 cm × 1 cm × 0.1 cm. The sample was ground with emery papers, cleaned with acetone and distilled water to remove products that might stick to the sample, and air-dried. The 1 M H_2SO_4 solution was prepared by diluting analytical-grade sulphuric acid with double-distilled water. The avocado used in this study was collected from a local plantation in the Gauteng region, South Africa. The avocado seed extraction was performed. Dried avocado seed powder, 500 g, was extracted with methanol in maceration for seven days. The macerated extract was filtered. The filtrate was collected while the residue was re-extracted with ethanol for seven days and then filtered again. The filtrate was concentrated using a rotary evaporator (Sigma-Aldrich, Bangalore, India) to obtain the concentrated extract. The concentrated extract was air-dried to remove the solvent. The inhibitor solutions were prepared from this stock solution with different concentrations of 1, 2, 3, 4, and 5 g/L, respectively, as the test solutions. This synthetic process was reported elsewhere [16]. The test solution was freshly prepared for each experiment.

Table 1. The API X65 pipeline steel chemical composition.

Element	Si	C	Ni	Nb	Cu	Al	Mn	P	S	Fe
Composition (wt.%)	0.186	0.09	0.016	0.023	0.01	0.016	0.867	0.006	0.003	Balance

2.2. Weight Loss Measurement

The X65 steel samples that were weighed and previously recorded were dipped into 250 mL of 1 molar sulphuric acid solution in the absence and presence of various avocado seed extract (ASPE) concentrations (1, 2, 3, 4, and 5 g/L) for an exposure time of 360 h at room temperature. A hole was drilled in the weight loss samples to enable the insertion of a hanger. The specimen was further polished with silicon carbide abrasive papers (400–1600), degreased in ethanol, air-dried, precisely weighed, and stored in a moisture-free desiccator before use to avoid atmospheric air. After 24 h intervals, the sample was cleaned with soft brushes, cleaned with distilled water, air-dried, and accurately re-weighed. Each experiment was performed in triplicate, and mean values were used to ensure the reproducibility of the result. From the obtained weight loss, the surface coverage, corrosion rate, and inhibition efficiency were computed.

2.3. Measurement of Potentiodynamic Polarization

A controlled Metrohm Autolab potentiostat/galvanostat NOVA 2.1.5 software (Metrohm, Pretoria, South Africa) was used in this study. The efficiency analysis of ASPE was conducted with the potentiodynamic polarization curve and linear polarization resistance techniques in a three-electrode glass cell. For the potentiodynamic polarization measurement, API 5L X65 steel was used as working electrodes with a 1 cm^2 exposed area, Ag/AgCl was used as the reference electrode, and platinum rods were used as counter electrodes. The test was conducted in 1 M sulfuric acid solution with and without ASPE. The electrode was immersed in the corrosive vessels with and without the ASPE. The corrosion current density value was calculated by Tafel extrapolation. To ensure the reproducibility and accuracy of the data, all tests were repeated three times.

2.4. Surface Study

2.4.1. Fourier-Transform Infrared (FTIR) Analysis

The characterization of the avocado seed extract was executed by FTIR (Shimadzu Corporation, Tokyo, Japan). FTIR measurement was conducted on the corrosion product, and FTIR measurement was also conducted for avocado seed extract.

2.4.2. Scanning Electron Microscopy/Energy-Dispersive Spectroscopy (SEM/EDX) Analysis

Surface analysis of the X65 steel samples with and without the optimum ASPE concentration at 298 K was examined using SEM (Oxford Instruments Plc, Oxfordshire, UK). The chemical analysis of the corrosion product was conducted using EDX analyzer (Oxford Instruments Plc, Oxfordshire, UK).

3. Result and Discussion

3.1. Gravimetric Measurement

The weight loss tests were conducted to examine the influence of ASPE on X65 steel in 1 M H_2SO_4 solutions with and without the extract for 360 h at 298 K. Diverse doses of the ASPE were injected into the experimental solutions to estimate the inhibition performance. Figures 1–4 show the effects of ASPE on the corrosion rates and inhibitive performance as a function of exposure time. According to Figures 1–4, increasing the ASPE extract concentration decreased the corrosion rates, increased the inhibitor's efficiency, and increased the surface coverage, denoting that increased ASPE concentration led to a high adsorption degree [26]. This denotes that ASPE was adsorbed on the X65 steel surface cover and inhibited the corrosion ions' aggressiveness on the surface of the X65 steel. This affirmation is also in agreement with the previous studies [27]. An increase in the ASPE concentration increased the ASPEs' efficiency; this observation might be due to the increase in charge and mass transfers to the metal surface, resulting in the inhibitor molecule adsorption and reduced metal dissolution. The maximum inhibitive efficiency of 88% occurred at 5 g/L. The basis of the inhibition process was the adsorption of the avocado seed extract molecules on the active sites and/or the deposition of the corrosion products

on the surface of metal [28]. As the inhibition efficiency increased with the addition of the inhibitor, a larger number of ASPE molecules were adsorbed on the surface of the metal, leading to a higher coverage of the surface [29]. At this point, there was a sharp decrease in the first part of the curve, which indicated that without ASPE, corrosion was in a free flow. However, the ASPE slowed down the corrosion process significantly, resulting in the observed curve. The observed high ASPE efficiency was, perhaps, owing to the SO_4^{2-} being hydrated in the sulphuric acid and being inadequately adsorbed to the surface of the metal, leaving a more active site for the ASPE adsorption; hence, the ASPE efficiency increased with the ASPE concentration. Therefore, it can be concluded that with the presence of ASPE in the H_2SO_4 solutions, the unshared electron pairs present on the various hetero atoms and the anions present in the inhibitor solutions were adsorbed on the steel surface. This observation also confirms the work of the study in [30].

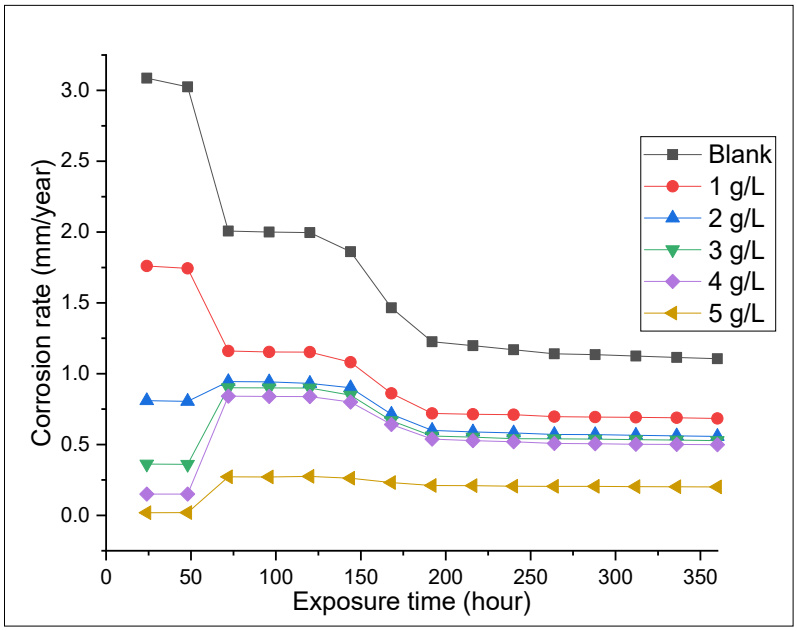

Figure 1. Corrosion rate against the exposure time at different concentrations.

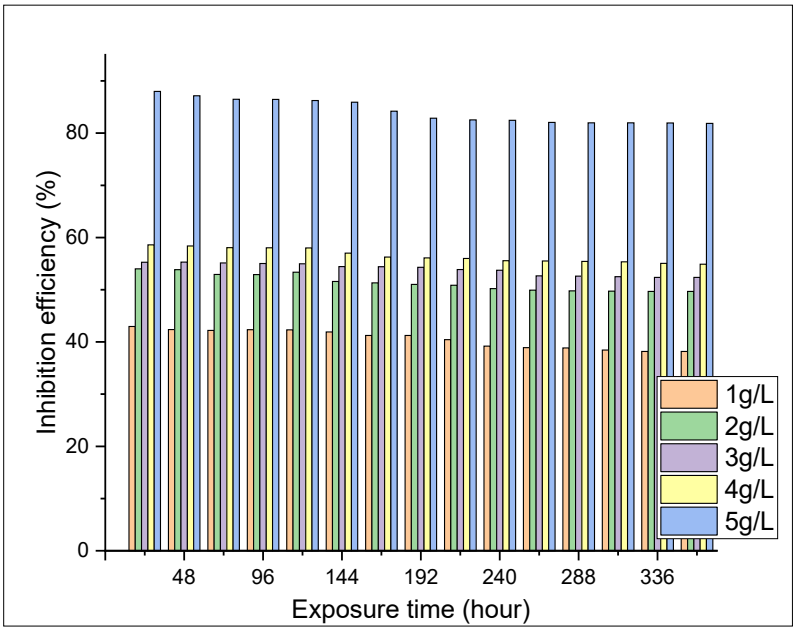

Figure 2. Inhibition efficiency against the exposure time at different concentrations.

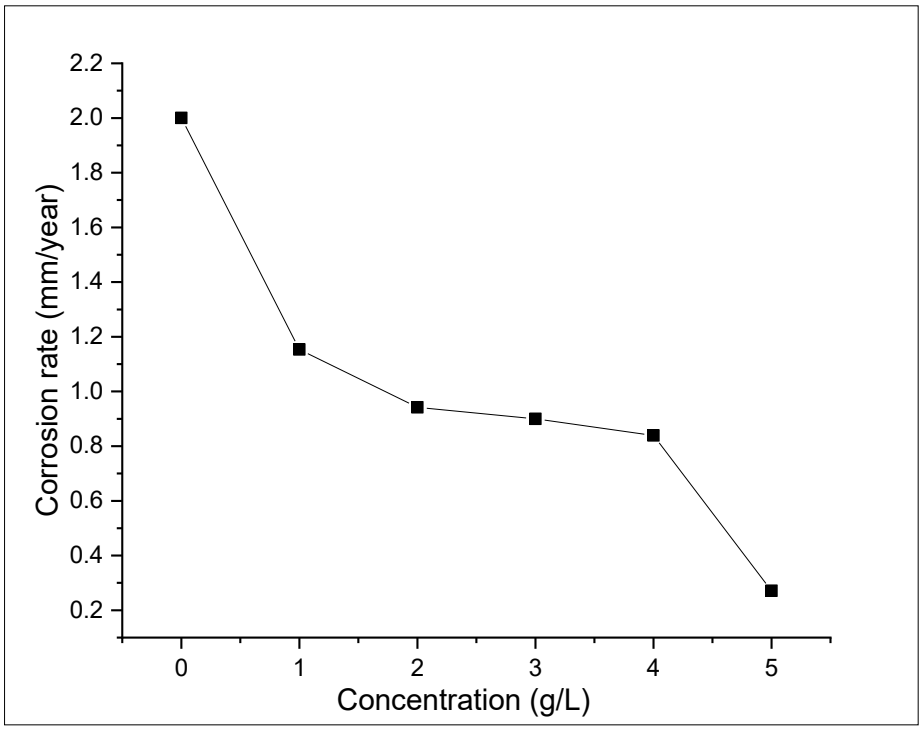

Figure 3. Variation in ASPE concentration based on the corrosion rate of X65 steel after 96 h.

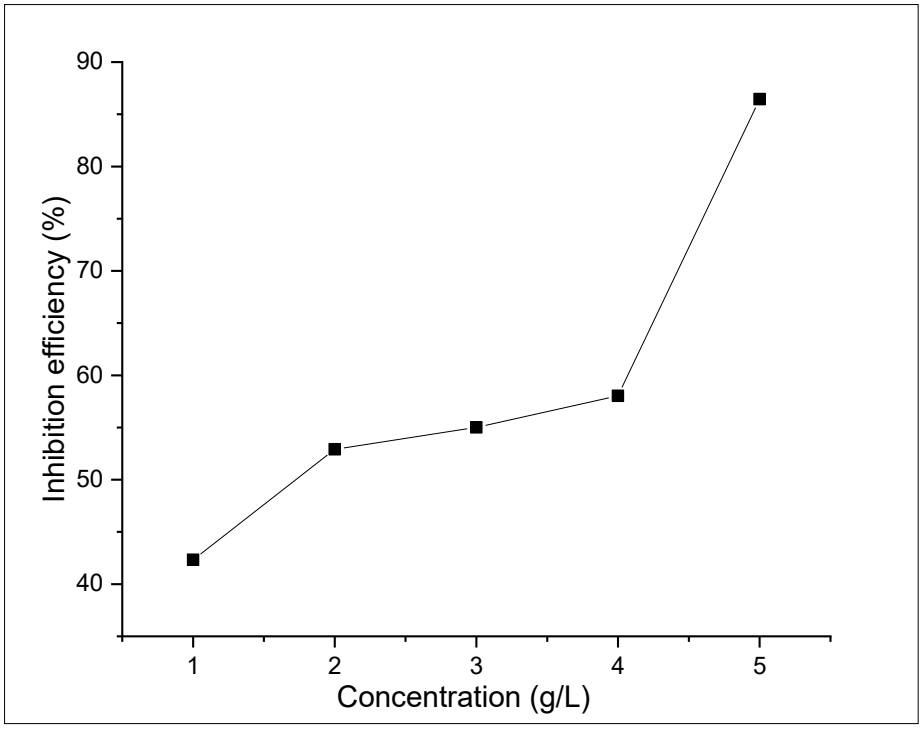

Figure 4. The effect of the inhibitor concentration on the inhibition efficiency after 98 h of immersion.

3.2. Potentiodynamic Polarization Method

The polarization curves for the X65 steel in 1 molar H_2SO_4 solution at diverse inhibitor concentrations are given in Figure 5. The Figure shows clearly that the presence of ASPE reduced the anodic and cathodic metal reactions to lower corrosion current density values, therefore causing an obvious decrease in the corrosion rate value. This performance revealed the inhibitive performance of ASPE. The electrochemical parameters, such as

corrosion potential (Ecorr), anodic and cathodic Tafel slopes (βa and βc), and current densities (Icorr), are shown in Table 2. The Table denotes that the ASPE reduced the current density and corrosion rate. This was due to the layer formed on the X65 steel by the extracts that inhibited the corrosion process [31]. Small changes in βa and βc denote that the corrosion mechanisms did not change with the ASPE [32]. The change in Ecorr values between the uninhibited and inhibited solution was less than 85 mV, indicating that the ASPE is a mixed-type inhibitor [33]. Increased ASPE concentrations led to irregularities in the anodic polarization current (overlapping). The irregularity observed in the anodic region was probably due to variation effects in the adsorbed ASPE on the surface. The most probable variation effect of the ASPE inhibitor, which is responsible for overlapping in the anodic current, was the protonation process. Hence, unprotonated and protonated species of ASPE could exist in the acid solution. Due to electrostatic attraction, the cationic species adsorbed onto the cathodic area of the steel and reduced the evolution of hydrogen, thereby protecting the cathodic sites of steel. The adsorption of ASPE at anodic sites could be attributed to the presence of unprotonated molecular species. An increase in the inhibitor concentration probably increased the number of protonated species on the surface [34]. Thus, it decreased the cathodic currents and limited the decrease in the anodic currents (with overlapping behavior). This could explain the strange ASPE anodic behavior observed at different concentrations. When this phenomenon was more prevalent than protonation, there was a decrease in the anodic current. The addition of ASPE decreased both cathodic and anodic Tafel slopes, confirming the mixed-type nature of the ASPE, thus affecting anodic steel dissolutions and the cathodic hydrogen evolution reaction.

Table 2. Electrochemical parameters for the API X65 steel in 1 M H_2SO_4 solution.

Inhibitor Concentration (g/L)	βa (V/dec)	βc (V/dec)	Ecorr (V)	Icorr (A/cm^2)	Polarization Resistance (Ω)	Corrosion Rate (mm/Year)	Eff_{100} Error (%0)
Blank	0.0424	0.1612	−0.3699	6.46×10^{-3}	22.583	7.5068	
1	0.0658	0.0709	−0.3686	3.23×10^{-3}	45.855	3.7570	15.5
2	0.0931	0.0282	−0.3675	2.29×10^{-3}	41.041	3.1340	11.9
3	0.0128	0.0089	−0.3663	2.12×10^{-3}	47.877	2.6599	10.1
4	0.0896	0.4833	−0.3605	4.75×10^{-5}	77.808	0.5520	8.7
5	0.0747	0.1369	−0.0146	1.34×10^{-7}	2452.6	0.0155	5.9

The error in efficiency can be determined using the method of propagation of errors. The errors can be calculated via the equations reported in [35]:

$$\Delta Eff = \left|\frac{\partial Eff}{\partial I_0}\right| \Delta I_0 + \left|\frac{\partial Eff}{\partial I_0}\right| \Delta I^I{}_0 \quad (1)$$

where ΔI_0 and $\Delta I^I{}_0$ are the experimental errors in the measurement of the current in the absence and presence of the inhibitor.

The errors calculated demonstrated that measuring any inhibition efficiency could have large errors associated with it, with the magnitude generally decreasing where efficiencies approached 100%. The major source of error for poorly performing inhibitors was the ability to reproducibly prepare the electrodes between each experiment, as seen in Table 2. This decreased the importance of errors associated with inconsistencies in surface preparation and enabled the reproducibility of the inhibition efficiency, predicted by the rapid screening technique, to approach 15%. The low errors for highly effective inhibitors provided good evidence to suggest that the rapid screening approach could ensure that effective corrosion inhibitors were not missed. Data for a wide number of inhibitors demonstrated a measured efficiency greater than 75%. Using the methodology presented in this

work, three repeat experiments were performed at varying inhibitor concentrations, and thus, the probability of overlooking a good inhibitor was further decreased.

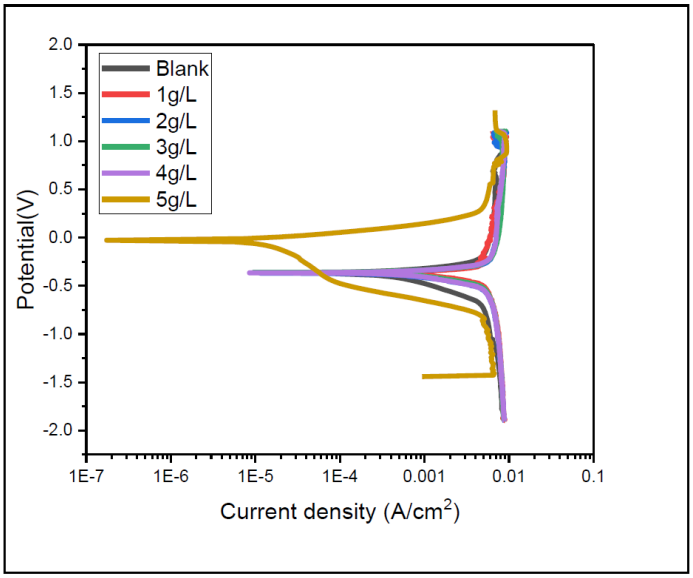

Figure 5. Potentiodynamic polarization curves of API X65 steel in 1 M H_2SO_4 in the presence and absence of APSE.

Linear Polarization Resistance (Rp) Readings

Polarization resistance is inversely proportional to the current density value, according to the Stern–Geary equation. Therefore, the smaller the Icorr values are, the higher the Rp values. Table 2 shows that for the blank sample, the Rp value was very low (22.58 Ω), denoting that the corrosion products formed on the surface of the X65 steel were not protected in the sulphuric acid solution. On the other hand, with the addition of ASPE, the Rp values monotonically increased as the ASPE concentration increased, due to the ASPE adsorbed. The reduction in the Rp value was due to the Fe^{2+} ion released during the anodic iron dissolution and the desorption of the layer formed by the ASPE. The high Rp value obtained with the 5 g/L concentration of ASPE corresponded with the results obtained with the polarization curve. The electrostatic connection between the metal surface and inhibitor molecules or the π-electron interactions with the steel are usually acceptable means by which inhibitors are adsorbed onto the surface of the metal. However, it is well-known in literature that the inhibitor behavior also depends on its structure, including the presence of unsaturated chains and the hydrophobic chain length. The inhibitive property of this organic compound is related to the unsaturated chains present that improve the adsorption of the inhibitor or the increased carbon atom number in the alkyl chain because the ASPE promotes the flat adsorption type, which decreases the active site present, blocking the adsorbed, aggressive species. Therefore, the long hydrophobic chain present makes ASPE highly effective.

3.3. Surface Morphology

The X65 steel surface morphology in one molar sulphuric acid solution with and without 5 g/L ASPE after the weight loss test was examined by SEM. The as-received morphology of the X65 steel sample, with and without ASPE, is presented in Figure 6. The sample in Figure 6a was without any indentations except the polished surface, and a completely smooth surface was revealed. In Figure 6b, the corrosion product layer formed showed the occurrence of the micro-crack path formed for the corrosive environments to corrode and penetrate the metal. It was obvious that the rate of resistance to corrosion decreased, which affirmed that the gravimetric result agreed with the potentiodynamic polarization result. A similar observation was previously reported [32]. With ASPE

(Figure 6c), the SEM micrograph showed a smooth and nonporous surface. The film formed on the steel surface was highly compact, compared to the blank sample, with minimal micro-cracks. Hence, it was highly protected. This was due to the material surface being covered by ASPE, forming a protective layer. The formed layer was caused by the interaction between the steel and the functional groups of compounds in ASPE. EDX examination showed the existence of Fe, C, and O for the corroded steel sample without PASE (Figure 6b). However, the O and C amounts increased for the corroded sample with 5 g/L PASE (Figure 6c), mainly due to the chemical elements present in the PASE. Steel material protection using extracts was considered an intermolecular synergistic effect of different extract components. This compound was rich in heteroatoms and aromatic rings to facilitate the molecule adsorption on the material surface by forming barriers that protect the metal against attacks from aggressive ions.

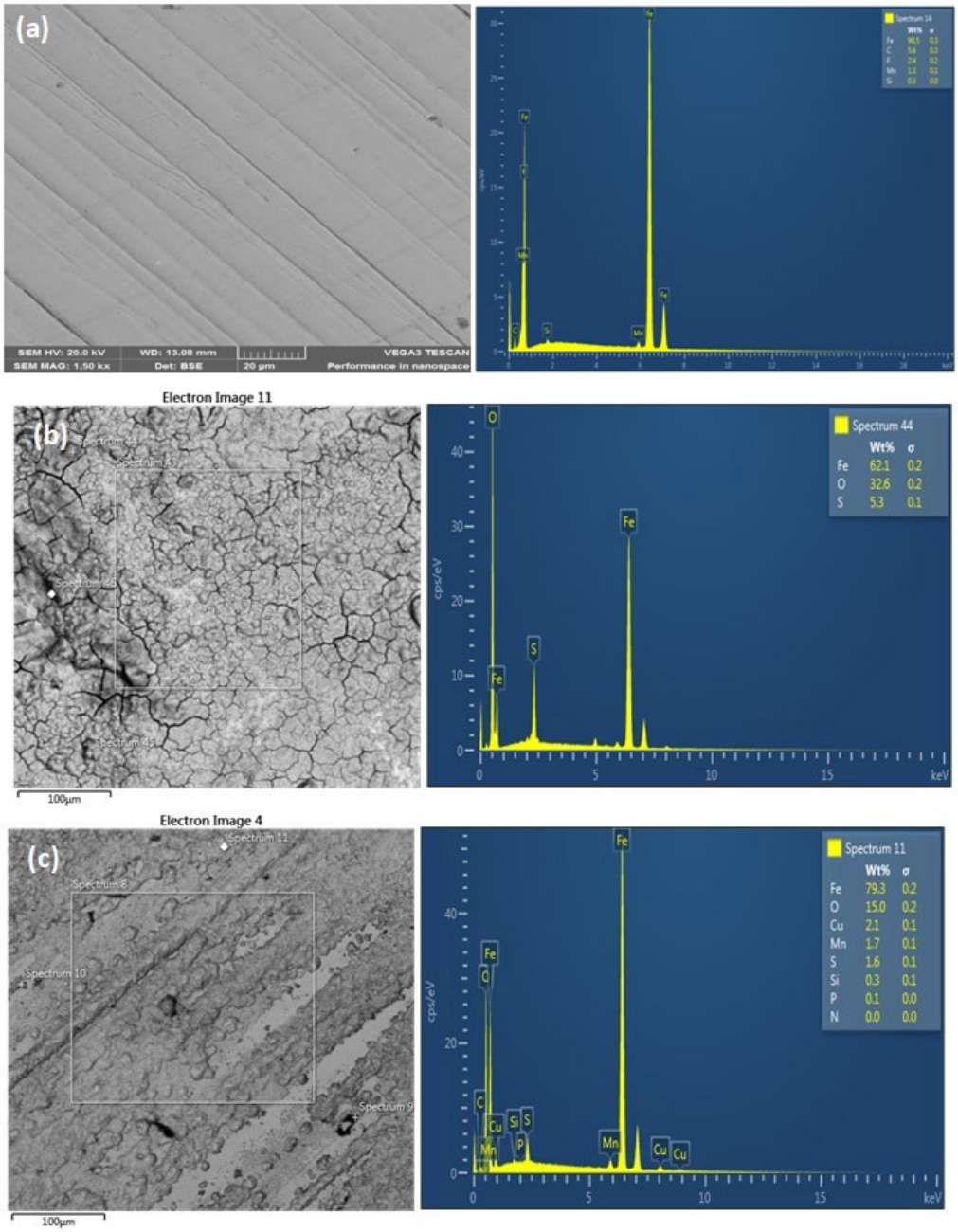

Figure 6. SEM/EDX analysis for the X65 steel surface before the corrosion test (**a**), X65 steel after the corrosion test without ASPE (**b**), and X65 steel after the corrosion test with 5 g/L ASPE (**c**).

3.4. FTIR Analysis

The FTIR study was utilized for the identification of functional groups that acted as inhibitors in the ASPE (Figure 7). Compounds that can be utilized as corrosion inhibitors are compounds with carboxyl, hydroxyl functional groups, carbonyl, amines, and other electron pairs that can interact with iron on the surface of the steel. The constituent can be adsorbed onto the metal surface by reducing the hydrogen gas evolution at the cathode or by blocking the active corrosion site. At wave number 1017 cm^{-1}, the absorption peak C=O was present. The wide peak of the O-H groups was indicated at 3304 cm^{-1}. Wave number 800 cm^{-1} denoted the aromatic C=C functional group. C=C alkene was at wave number 751 cm^{-1}, with sharp absorption peaks, and C=N was present at 2858 cm^{-1}, with a strong intensity and a sharp absorption peak. From the FTIR, ASPE had chemical functional groups that served as a green corrosion inhibitor. With similar results, Gusti et al., 2019 [21], concluded that the obtained compound from avocado seed was rich in polysaccharides, due to its functional groups, with a small quantity of tannin, among other compounds. Consequently, the derived inhibitor from avocado seed possibly contained nitrogen and oxygen atoms (Figure 8) in the aromatic ring and the functional group, which are generally found in other corrosion inhibitor structures with high inhibitory properties [25]. Figure 9 signifies a shift in the wave number, denoting the connection between the metal surfaces and the functional groups.

We examined the FTIR spectrum of the corroded layer on the X65 steel surface after the immersions in the H_2SO_4 solutions with and without 5 g/L ASPE to reveal the adsorption means of the ASPE molecule on the X65 steel (Figure 9). The main spectral regions identified for the as-received avocado seed extract were at ~1017 (arising from carbonyl C=O groups), ~1740 (due to O–H groups), ~751 and ~800 (due to C=C), and ~2858 (resulting from stretching ester C–N groups). Occurrence of peaks (with inhibitor) at the regions of ~3367 cm^{-1} (–O–H), ~663 cm^{-1} and ~1023 cm^{-1} (C=C), ~1618 cm^{-1} (C–O), and ~2361 cm^{-1} (C–N) indicated that the spectrum formed after the immersion tests in the corrosive solution upon the addition of ASPE. It can be seen that after the immersion tests, the concentrated band at the 3000–3500 cm^{-1} [36] region corresponded to the stretching of the O–H groups (~3367.76 cm^{-1}). The dominant features at 3000–2800 cm^{-1} and 1820–1660 cm^{-1} were attributed to the symmetric and asymmetric stretching vibrations of CH_2 and C O, respectively [37]. Therefore, the band at ~1618 cm^{-1} arose predominantly from the ester C–O groups. The peaks at the regions 650–750 cm^{-1} and 1300–1000 cm^{-1} corresponded to ester C–O–C stretching vibrations and –CH CH– bonds, respectively. Upon the addition of ASPE, the peaks present in the 1660–2400 cm^{-1} region arose from C–N groups (~2361 cm^{-1}). The peaks at ~1618 cm^{-1} (C–O) in the acidic solution could be attributed to aldehyde carbonyl and ester carbonyl groups that were mutually overlapped. However, in both sediments, narrowing the C–O peak at ~1618 cm^{-1} indicated less concentrations of carbonyl groups. The formation of nitrogen-bearing compounds was evidenced in the FTIR spectrum of the residues, which exhibited broad transmittance centered at ~2361 cm^{-1} (C–N) in high concentrations. A positive correlation for the peaks at ~2361–3367 cm^{-1} in the sediments would imply that the nitrogen groups associated with these peaks were constituents of ASPE formed on the steel surface in the acid solution. This variation might be caused by the contact between PASE molecule constituents and the X65 steel, resulting in the formed protective layers.

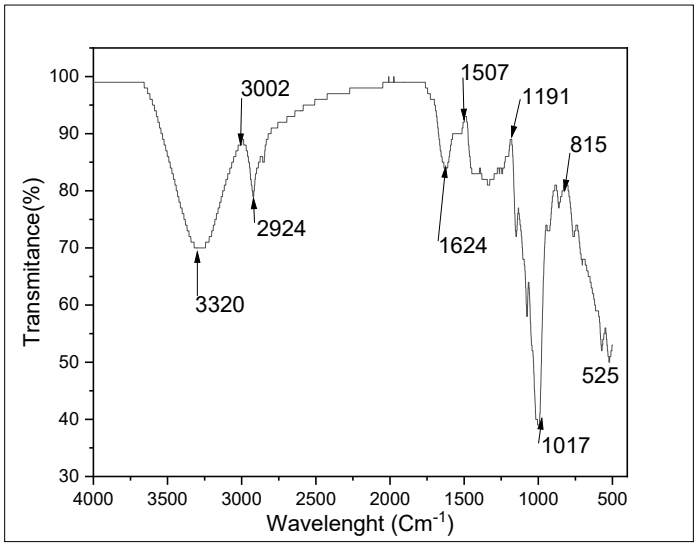

Figure 7. FTIR spectrum of the avocado seed extract used in this study.

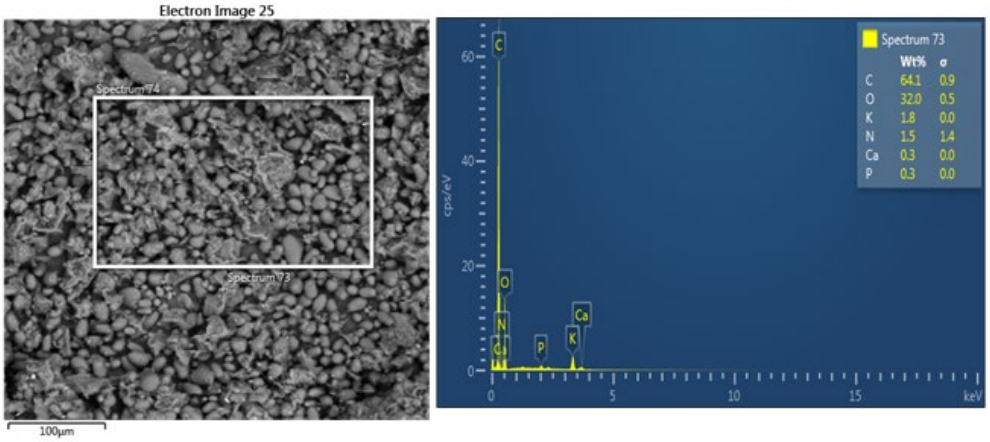

Figure 8. SEM/EDX analysis of the avocado seed extract.

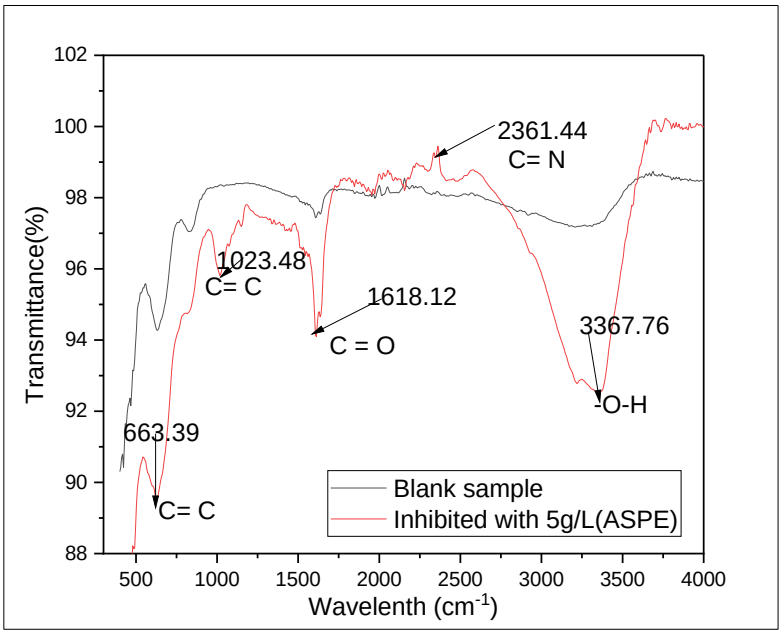

Figure 9. FTIR spectra of the ASPE-formed films on the X65 steel.

3.5. Adsorption Isotherms

Adsorption isotherm was used for establishing significant insight on the relationship between the X65 steel surface and the ASPE extract as shown in Figure 10. The ASPE molecule replacement for the water molecules occurred during the ASPE adsorption on the X65 steel surface, based on the adsorption concept. Therefore, the obtained data from the gravimetric result were used to simulate different isotherms, including Flory–Huggins, Langmuir, Tempkin, and Frumkin. The adsorption isotherm that had the best fit among the various models, with the correlation coefficient R^2 = 0.99, was the Langmuir one, which ascertained a protecting mono-layer of ASPE molecules on the X65 steel. Equation (2) assumes water molecule displacement from the X65 steel by the ASPE molecule adsorbed:

$$\frac{C}{\theta} = \frac{1}{K_{ads}} + C \tag{2}$$

where C is the inhibitors' concentrations, and K_{ads}, and θ are the adsorption equilibrium constant and the degree of surface coverage, respectively.

The calculated K_{ads} was estimated to be 5.47×10^6 (mg/L). The K_{ads} was related to the standard free adsorption energy ($\Delta G^0{}_{ads}$), according to Equation (3):

$$\Delta G^o{}_{ads} = -RT \ln(K_{ads}) \tag{3}$$

where T is the absolute temperature, and R is the universal gas constant.

This led to a free-energy adsorption value of −29.33 kJ/mol. The higher the negative value of $\Delta G^0{}_{ads}$, the stronger the connection between the inhibitor and the steel. Therefore, a value of approximately −20 kJ mol^{-1} for $\Delta G^0{}_{ads}$ denoted physical interactions amid the metal and the inhibitor. Therefore, the energy adsorption value of −29.33 kJ mol^{-1} denoted that ASPE was adsorbed physically onto the X65 steel surface.

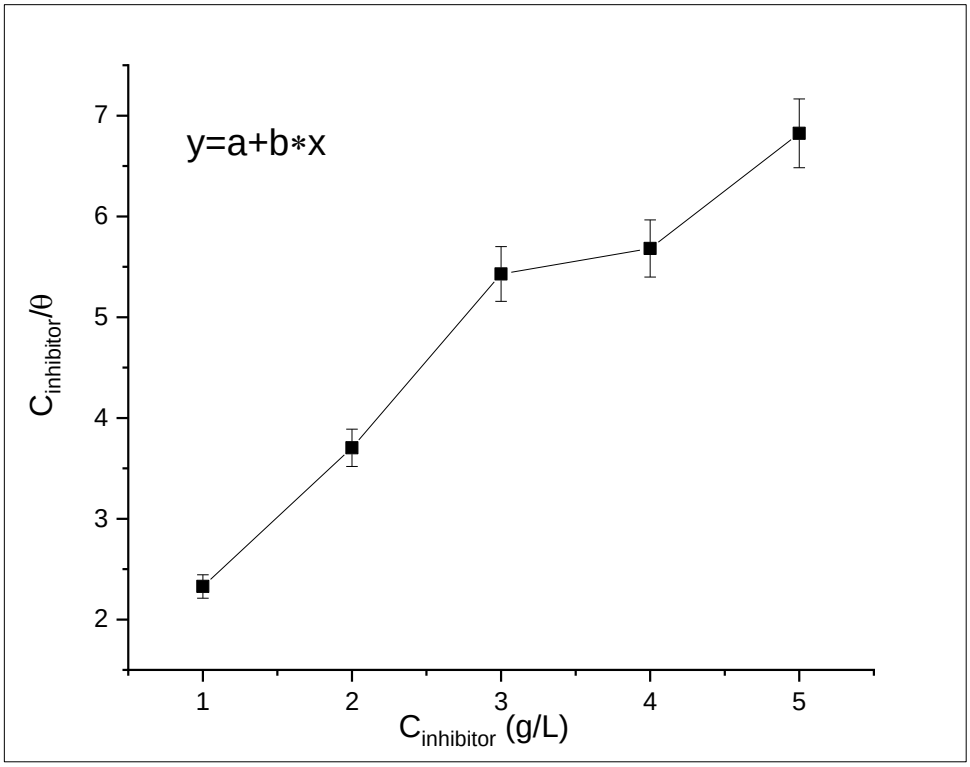

Figure 10. The Langmuir adsorption isotherms for X65 steel in 1 M H_2SO_4 solutions at different ASPE concentrations.

4. Conclusions

The avocado seed extract is a biomass that is commonly available. Therefore, the avocado seed extract was investigated for X65 pipeline steel, as they are cost-effective, more environmentally benign, and less toxic via electrochemical and gravimetric techniques, including SEM, EDX, and FTIR analysis. From this study, the following conclusions were drawn:

(1) The FTIR spectrum result demonstrated that the ASPE had components generally established in green inhibitors; heteroatoms, for instance, oxygen and nitrogen (C–H, C=O, C–O, O–H, N–H), and an aromatic ring that could be adsorbed to the surface of the metal built barriers that shielded the metal from corroding.
(2) The corrosion rate decreased, and the inhibition efficiency increased on the X65 steel with increasing ASPE concentrations, with an optimum efficiency of 88% at 5 g/L.
(3) ASPE was classified as a mixed inhibitor; the adsorption isotherms showed that the process fit the Langmuir isotherm.
(4) The SEM/EDX analysis of the protective film adsorbed on the X65 steel affirmed the high inhibitive behavior of the active component in the ASPE. Therefore, avocado seed powder is a promising inhibitor. This study reveals a new avenue for non-toxic inhibitors for X65 pipeline steel.

Author Contributions: Conceptualization, A.O.A.; formal analysis, O.S.; methodology, A.O.A.; resources, A.P.P.; supervision, O.S. and A.P.P.; validation, A.P.P.; writing—original draft, A.O.A.; writing—review and editing, O.S. All authors have read and agreed to the published version of the manuscript.

Funding: This research received no external funding.

Data Availability Statement: Data are unavailable in this study.

Acknowledgments: The authors would like to thank the Surface Engineering Research Laboratory (SERL) at Tshwane University of Technology in Pretoria for providing laboratory equipment and technical help.

Conflicts of Interest: The authors declare no conflict of interest.

References

1. Alamri, A.H. Localized corrosion and mitigation approach of steel materials used in oil and gas pipelines—An overview. *Eng. Fail. Anal.* **2020**, *116*, 104735. [CrossRef]
2. Lieth, H.M.; Al-Sabur, R.; Jassim, R.J.; Alsahlani, A. Enhancement of corrosion resistance and mechanical properties of API 5L X60 steel by heat treatments in different environments. *J. Eng. Res.* **2021**, *9*, 428–440. [CrossRef]
3. Haruna, K.; Alhems, L.M.; Saleh, T.A. Graphene oxide grafted with dopamine as an efficient corrosion inhibitor for oil well acidizing environments. *Surf. Interfaces* **2021**, *24*, 101046. [CrossRef]
4. Sanni, O.; Popoola, A.P.I.; Fayomi, O.S.I. Enhanced corrosion resistance of stainless steel type 316 in sulphuric acid solution using eco-friendly waste product. *Results Phys.* **2018**, *9*, 225–230. [CrossRef]
5. Da Silva, R.F.; Carneiro, C.N.; de Sousa, C.B.D.C.; Gomez, F.J.; Espino, M.; Boiteux, J.; Fernández, M.D.L.Á.; Silva, M.F.; Dias, F.D.S. Sustainable extraction bioactive compounds procedures in medicinal plants based on the principles of green analytical chemistry: A review. *Microchem. J.* **2022**, *175*, 107184. [CrossRef]
6. Carvalho, M.C.F.D.; Almeida, N.M.S.D.; Silva, I.M.F.C.R.; Cotting, F.; Aoki, I.V.; Capelossi, V.R. Electrochemical and Economic Evaluation of the Cocoa Bean Shell as a Corrosion Inhibitor in Acidic Medium. *Mater. Res.* **2022**, *25*, e20210125. [CrossRef]
7. Popoola, L.T.; Aderibigbe, T.A.; Lala, M.A. Mild Steel Corrosion Inhibition in Hydrochloric Acid Using Cocoa Pod Husk-Ficus exasperata: Extract Preparation Optimization and Characterization. *Iran. J. Chem. Chem. Eng.* **2022**, *41*, 482–492.
8. Olasehinde, E.F.; Agbaffa, E.B.; Adebayo, M.A.; Abata, E.O. Corrosion Inhibition of Mild Steel in 1 M HCl by Methanolic Chromolaena odorata Leaf Extract: Experimental and Theoretical Studies. *J. Bio- Tribo-Corros.* **2022**, *8*, 105. [CrossRef]
9. Tan, B.; Xiang, B.; Zhang, S.; Qiang, Y.; Xu, L.; Chen, S.; He, J. Papaya leaves extract as a novel eco-friendly corrosion inhibitor for Cu in H_2SO_4 medium. *J. Colloid Interface Sci.* **2021**, *582*, 918–931. [CrossRef]
10. Harb, M.B.; Abubshait, S.; Etteyeb, N.; Kamoun, M.; Dhouib, A. Olive leaf extract as a green corrosion inhibitor of reinforced concrete contaminated with seawater. *Arab. J. Chem.* **2021**, *13*, 4846–4856. [CrossRef]
11. Chen, S.; Zhu, B.; Liang, X. Corrosion inhibition performance of coconut leaf extract as a green corrosion inhibitor for X65 steel in hydrochloric acid solution. *Int. J. Electrochem. Sci.* **2020**, *15*, 1. [CrossRef]

12. Da Silva, M.V.L.; de Britto Policarpi, E.; Spinelli, A. Syzygiumcumini leaf extract as an eco-friendly corrosion inhibitor for carbon steel in acidic medium. *J. Taiwan Inst. Chem. Eng.* **2021**, *129*, 342–349. [CrossRef]
13. Furtado, L.B.; Nascimento, R.C.; Guimaraes, M.J.O.; Henrique, F.J.; Rocha, J.C.; Seidl, P.R.; Gomes, J.A.C. Cleaner corrosion inhibitors using *Peumusboldus* Molina formulations in oil well acidizing fluids: Gravimetric, electrochemical and DFT studies. *Sustain. Chem. Pharm.* **2021**, *19*, 100353. [CrossRef]
14. Kreitzman, M.; Toensmeier, E.; Chan, K.; Smukler, S.; Ramankutty, N. Perennial staple crops: Yields, distribution, and nutrition in the global food system. *Front. Sustain. Food Syst.* **2021**, *4*, 216. [CrossRef]
15. FAO. *Major Tropical Fruits—Preliminary Market Results 2019*; FAO: Rome, Italy, 2020.
16. Cruz-Zabalegui, A.; Vazquez-Velez, E.; Galicia-Aguilar, G.; Casales-Diaz, M.; Lopez-Sesenes, R.; Gonzalez-Rodriguez, J.G.; Martinez-Gomez, L. Use of a non-ionic gemini-surfactant synthesized from the wasted avocado oil as a CO_2-corrosion inhibitor for X-52 steel. *Ind. Crops Prod.* **2019**, *133*, 203–211. [CrossRef]
17. Sanni, O.; Popoola, A.; Fayomi, O. Adsorption ability and corrosion inhibition mechanism of agricultural waste on stainless steel in chloride contaminated environment. *Mater. Today Proc.* **2021**, *43*, 2215–2221. [CrossRef]
18. Sun, X.; Qiang, Y.; Hou, B.; Zhu, H.; Tian, H. Cabbage extract as an ecofriendly corrosion inhibitor for X70 steel in hydrochloric acid medium. *J. Mol. Liq.* **2022**, *362*, 1119733. [CrossRef]
19. Zakaria, F.A.; Hamidon, T.S.; Hussin, M.H. Applicability of winged bean extracts as organic corrosion inhibitors for reinforced steel in 0.5 M HCL electrolyte. *J. Indian Chem. Soc.* **2022**, *99*, 100329. [CrossRef]
20. De Jesus, M.E.S.; de Mendonça Santos, A.; Tokumoto, M.S.; Cotting, F.; Aquino, I.P.; Capelossi, V.R. Evaluation of Efficiency of avocado seed powder (*Persea Americana*) as a corrosion inhibitor in SAE 1008 carbon steel in acidic medium. *Braz. J. Dev.* **2020**, *6*, 77197–77215.
21. Gusti, D.R.; Lestari, I.; Farid, F.; Sirait, P.T. Protection of mild steel from corrosion using methanol extract of avocado (*Persea americana mill*) seeds in a solution of sulfuric acid. *J. Phys. Conf. Ser.* **2019**, *1282*, 012083. [CrossRef]
22. Mu'azu, K.; Aliyu, M.M.; Mohammed, A.T.; Lasisi, S.; Dahiru, R.; Suleiman, I.Y. Ethanol Extract of Avocado Leaf as Corrosion Inhibitor for the Protection of Mild Steel in Acidic Environment. *J. Mater. Environ. Sci.* **2022**, *13*, 1343–1354.
23. Ehiemere, A.C.; OnyekachiAnyanwu, R.; Emele, P.; Nwokeke, U.G. Anti-corrosion potentials of fresh extracts of old *persea americana* seed in 0.5 M H_2SO_4 on mild steel. *Int. Inst. Sci. Technol. Educ. IISTE* **2021**, *13*, 2.
24. Radi, M.; Melian, R.; Galai, M.; Dkhirche, N.; Ech-chihbi, E.; Touhami, M.E. Performance of Avocado Seeds as New Green Corrosion Inhibitor for 7075-T6 Al Alloy in a 3.5% NaCl Solution: Electrochemical, Thermodynamic, Surface and Theoretical Investigations. *Port. Electrochem. Acta* **2023**, *41*, 425–445. [CrossRef]
25. Verma, D.K.; Dewangan, Y.; Dewangan, A.K.; Asatkar, A. Heteroatom-based compounds as sustainable corrosion inhibitors: An overview. *J. Bio- Tribo-Corros.* **2021**, *7*, 15. [CrossRef]
26. Vorobyova, V.; Skiba, M.; Gnatko, E. Agri-food wastes extract as sustainable-green inhibitors corrosion of steel in sodium chloride solution: A close look at the mechanism of inhibiting action. *S. Afr. J. Chem. Eng.* **2023**, *43*, 273–295. [CrossRef]
27. Sanni, O.; Popoola, A.P.I.; Fayomi, O.S.I. Temperature effect, activation energies and adsorption studies of waste material as stainless steel corrosion inhibitor in sulphuric acid 0.5 M. *J. Bio- Tribo-Corros.* **2019**, *5*, 88. [CrossRef]
28. Sengupta, S.; Murmu, M.; Murmu, N.C.; Banerjee, P. Adsorption of redox-active Schiff bases and corrosion inhibiting property for mild steel in 1 mol H_2SO_4: Experimental analysis supported by ab initio DFT, DFTB and molecular dynamics simulation approach. *J. Mol. Liq.* **2021**, *326*, 115215. [CrossRef]
29. Bidi, M.A.; Azadi, M.; Rassouli, M. A new green inhibitor for lowering the corrosion rate of carbon steel in 1 M HCl solution: Hyalomma tick extract. *Mater. Today Commun.* **2020**, *24*, 100996. [CrossRef]
30. Fouda, A.S.; El-Gharkawy, E.S.; Ramadan, H.; El-Hossiany, A. Corrosion resistance of mild steel in hydrochloric acid solutions by clinopodiumacinos as a green inhibitor. *Biointerface Res. Appl. Chem.* **2021**, *11*, 9786.
31. Sanni, O.; Iwarere, S.A.; Daramola, M.O. Evaluation of Corrosion Inhibition of Essential Oil-Based Inhibitors on Aluminum Alloys. *ACS Omega* **2022**, *7*, 40740–40749. [CrossRef]
32. Guo, W.; Umar, A.; Zhao, Q.; Alsaiari, M.A.; Al-Hadeethi, Y.; Wang, L.; Pei, M. Corrosion inhibition of carbon steel by three kinds of expired cephalosporins in 0.1 M H_2SO_4. *J. Mol. Liq.* **2022**, *320*, 114295. [CrossRef]
33. Konkena, B.; Vasudevan, S. Understanding aqueous dispersibility of graphene oxide and reduced graphene oxide through p *K* a measurement. *J. Phys. Chem. Lett.* **2012**, *3*, 867–872. [CrossRef]
34. Fazal, M.A.; Haseeb, A.S.M.A.; Masjuki, H.H. Corrosion mechanism of copper in palm biodiesel. *Corros. Sci.* **2013**, *67*, 50–59. [CrossRef]
35. Yeganeh, M.; Khosravi-Bigdeli, I.; Eskandari, M.; Alavi Zaree, S.R. Corrosion inhibition of L-methionine amino acid as a green corrosion inhibitor for stainless steel in the H_2SO_4 solution. *J. Mater. Eng. Perform.* **2020**, *29*, 3983–3994. [CrossRef]
36. Musa, A.Y.; Kadhum, A.A.H.; Mohamad, A.B.; Daud, A.R.; Takriff, M.S.; Kamarudin, S.K. A comparative study of the corrosion inhibition of mild steel in sulphuric acid by 4,4-dimethyloxazolidine-2-thione. *Corros. Sci.* **2009**, *51*, 2393–2399. [CrossRef]
37. Muster, T.H.; Hughes, A.E.; Furman, S.A.; Harvey, T.; Sherman, N.; Hardin, S.; Corrigan, P.; Lau, D.; Scholes, F.H.; White, P.A.; et al. A rapid screening multi-electrode method for the evaluation of corrosion inhibitors. *Electrochem. Acta* **2009**, *54*, 3402–3411. [CrossRef]